Supplementary Information for

A zero-strain Na-deficient NASICON-type $Na_{2.8}Mn_{0.4}V_{1.0}Ti_{0.6}(PO_4)_3$ cathode for wide-temperature rechargeable Na-ion batteries

Xing Shen [a, b], Yuefeng Su [a, b, *], Shunli He [b], Yali Li [b], Lifeng Xu [a b], Ni Yang [b], Yanshun Liao[a, b], Meng Wang [b] and Feng Wu[a, b, *]

[a]School of Materials Science and Engineering, Beijing Key Laboratory of Environmental Science and Engineering, Beijing Institute of Technology, Beijing 100081, China. *Email: suyuefeng@bit.edu.cn, wufeng863@bit.edu.cn

[b]Beijing Institute of Technology, Chongqing Innovation Center, Chongqing, 401120, China

Experimental section

Materials Preparation

$Na_{2x+2}Mn_xV_{1.0}Ti_{1-x}(PO_4)_3$ (x=0.4, 0.5, 0.6) cathode materials were prepared via a typical sol-gel method followed by a high temperature calcination process under Ar atmosphere. In a typical synthesis, stoichiometric amounts of sodium acetate, acetylacetone manganese, vanadium acetylacetonate, tetrabutyl titanate and phosphoric acid were added into the mixed solution consisting of ethanol and citric acid. Here, citric acid was used as both a chelating agent and carbon resource. After stirring for 2 hours at 90 ^{o}C, the solvent was almost evaporated with gel in the beaker. The gel was then transferred into the vacuum oven to obtain the dried powder. After that, the powder was subjected to a high temperature calcination (700 ^{o}C) for 4h to acquire the $Na_{2x+2}Mn_xV_{1.0}Ti_{1-x}(PO_4)_3$ serial materials.

Materials Characterizations

The crystal structure of the samples was characterized by an X-ray powder diffractometer (Rigaku SmartLab 9kw) using Cu-Kα1 radiation (1.5406 Å) at 40 kV and 40 mA. The micro-morphology and fine phase structure of the as-prepared samples were observed with a field emission scanning electron microscope (FESEM) (JEOL, JSM-7800FPRIME) and a high-resolution transmission electron microscope (HRTEM) (Thermo Fisher Scientific CDLtd, Talos F200S) equipped with energy-dispersive X-ray spectroscope (EDS), respectively. The element concentrations of Na, Mn, V, Ti and P were tested by

Inductively coupled plasma mass spectrometer (Agilent 7850 ICP-MS). The Brunauer-Emmett-Teller (BET) surface area and pore size distribution of samples were measured from a nitrogen adsorption isotherm analysis (Quantachrome, AUTOSORB-IQ-XR-C). Structure details and phase information of the as-prepared cathodes were characterized by Raman spectra (HORIBA, labRAM HR evolution) and Fourier-transform infrared spectroscopy (Bruker, Tensor 27). The element valence of samples and electrodes was determined by X-ray photoelectron spectroscopy (XPS) using Kratos AXIS SUPRA+.

Electrochemical measurements

To fabricate cathode electrodes, the active materials, super P and polytetrafluoroethylene (PTFE) binder were ground at a mass ratio of 8:1:1 until the formation of a uniformly distributed film. The composites were sliced into thin square electrodes with an active loading amount of 6-10 mg cm^2. Coin-type (CR2032) cells were assembled in an argon-filled glove box (MIKROUNA) full of Ar (the concentration of H_2O and O_2 are less than 0.1 ppm). The fresh Na foils were used as counter electrodes. A thin sheet of microporous glass fiber (Whatman GF/D) served as the separator. $NaClO_4$ electrolyte (1.0 M) in propylene carbonate (PC) solution with 2 wt% fluoroethylene carbonate (FEC) was used as the electrolyte. All the galvanostatic charge/discharge measurements under various current densities were carried out on a Land battery testing system at stated temperature. The voltage window is between

2.0 and 4.2 V. Cyclic voltammetry (CV) curves were recorded on an electrochemical workstation (CH Instruments, CHI660C). For the galvanostatic intermittent titration technique (GITT) measurement, the cell was charged with a low current at 0.1 C for 10 min followed by a relaxation period of 40 min. The electrochemical impedance spectroscopy measurements were carried out on the Zahner IM6 in the frequency range of 1 MHz to 10 mHz.

The calculation of pseudocapacitance contribution

The pseudocapacitance contribution can be calculated based on the following methods, First, get CV curves at various scan rates. Upon the same voltage range, the current at various scan rates was obtained and the b value (the slope of the curve) can be calculated according to **Equation (1):**

$i/v^{0.5} = \mathrm{b}v^{0.5} + \mathrm{a}$ **Equation (1)**

and then, get the b value at different potentials. Finally, we can get the capacitive contribution part current values at different potentials by b**v*.

The calculation of diffusion coefficient by the GITT method

Equation (2 is used to determine the diffusion coefficient of Na ions derived from Weppner et al, and the parameters needed can be obtained from GITT curves.

$$D_{Na^+} = \frac{4}{\pi\tau}\left(\frac{m_B V_M}{M_B S}\right)^2\left(\frac{\Delta E_s}{\Delta E_\tau}\right)^2 \qquad \left(\tau \ll L^2/D_{Na^+}\right)$$ **Equation (2)**

Where m_B and M_B are the mass and molecular weight of the NVP-based sample, respectively. V_M is the molar volume. τ is the pulse time. S is the active surface of the electrode. L represents the ion diffusion length. ΔE_s and ΔE_τ are the variations of quasi-equilibrium potential and transient potential during the current pulse, respectively.

The determination of activation energy (Ea) based on electrochemical impedance spectroscopy

Firstly, Nyquist plots of as-synthesized samples were tested at different temperatures. Here, we selected the temperatures of 0 ^oC, 25 ^oC and 55 ^oC. After that, fitting the EIS data with appropriate equivalent circuit to obtain the charge transfer resistance (R_{ct}) value. Based on the R_{ct} value, the corresponding ionic conductivity σ can be calculated as:

σ=L/RS **Equation (3)**

L represents the length of electrode sample, S stands for the cross sectional area of electrode. Then, the activation energy can be obtained according to the Arrhenius equation:

σ=Aexp(-Ea/KT) **Equation (4)**

Here, Ea represents the activation energy, T represents the absolute temperature, K stands for the Boltzmann constant, and A represents the pre-exponential factor. Take 1000/T as the X-axis with Inσ as the Y-axis, and the obtained slope can be regarded as the corresponding activation energy.

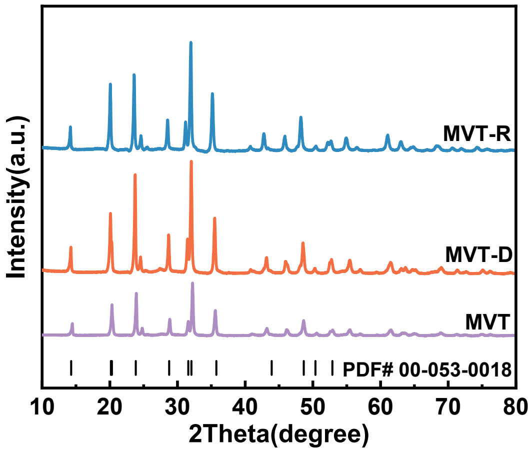

Figure S1 The XRD patterns of the as-prepared cathodes.

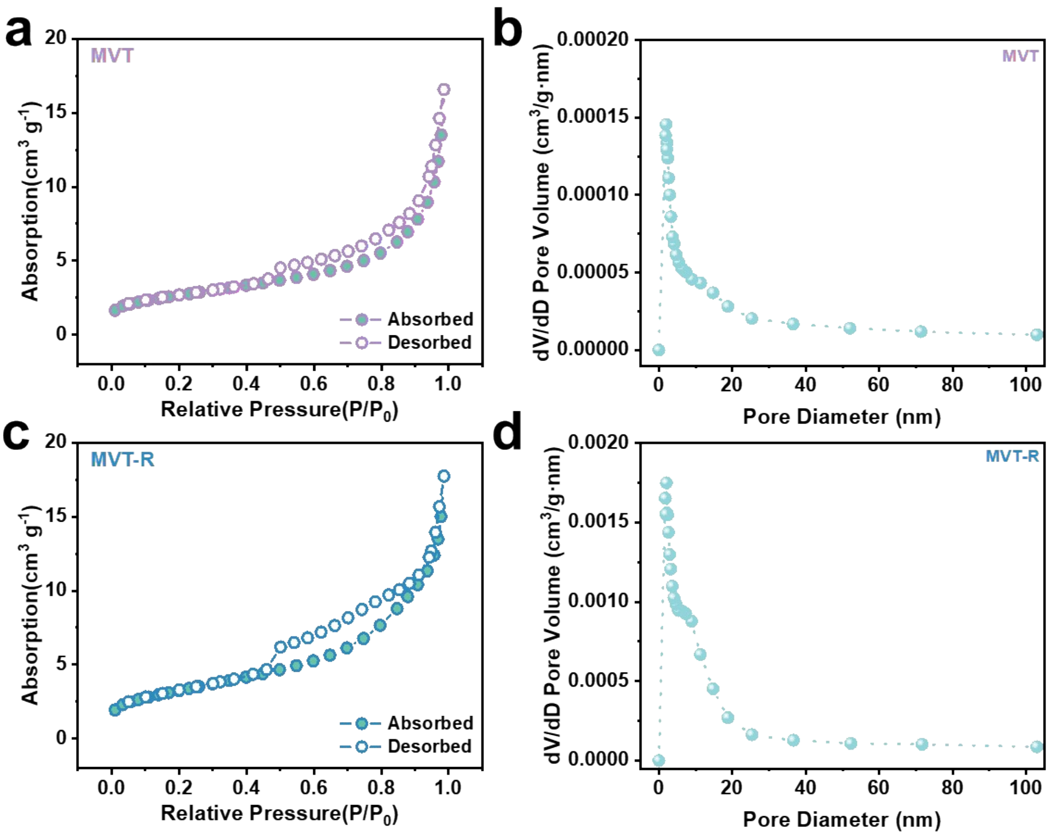

Figure S2 (a) The nitrogen adsorption-desorption curves and (b) the corresponding pore-size distribution of MVT cathode. (c) The nitrogen adsorption-desorption curves and (d) the corresponding pore-size distribution of MVT-R cathode.

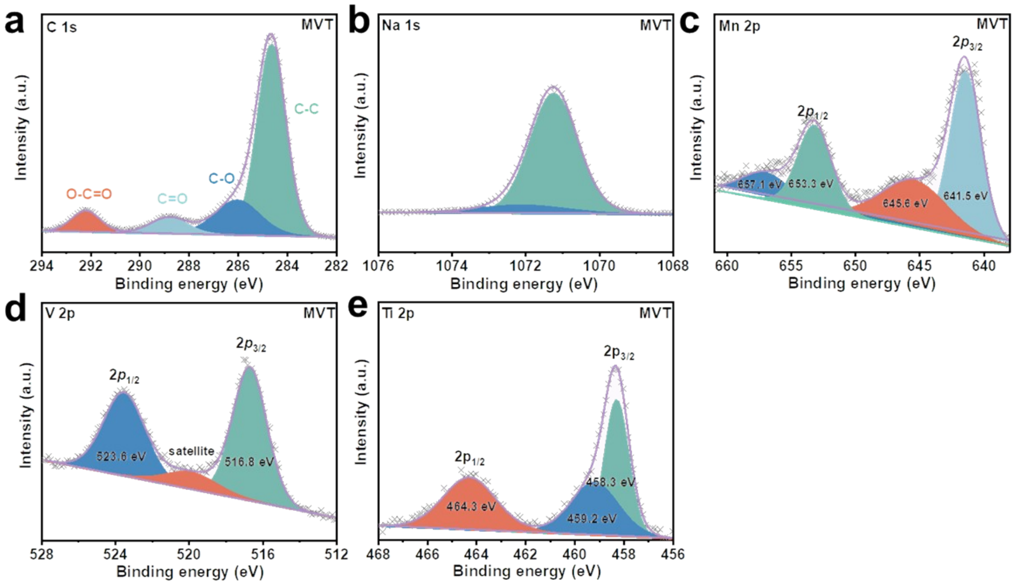

Figure S3 Fitted XPS spectra of (a) C 1s, (b) Na 1s, (c) Mn 2p, (d) V 2p and (f)Ti 2p for MVT cathode.

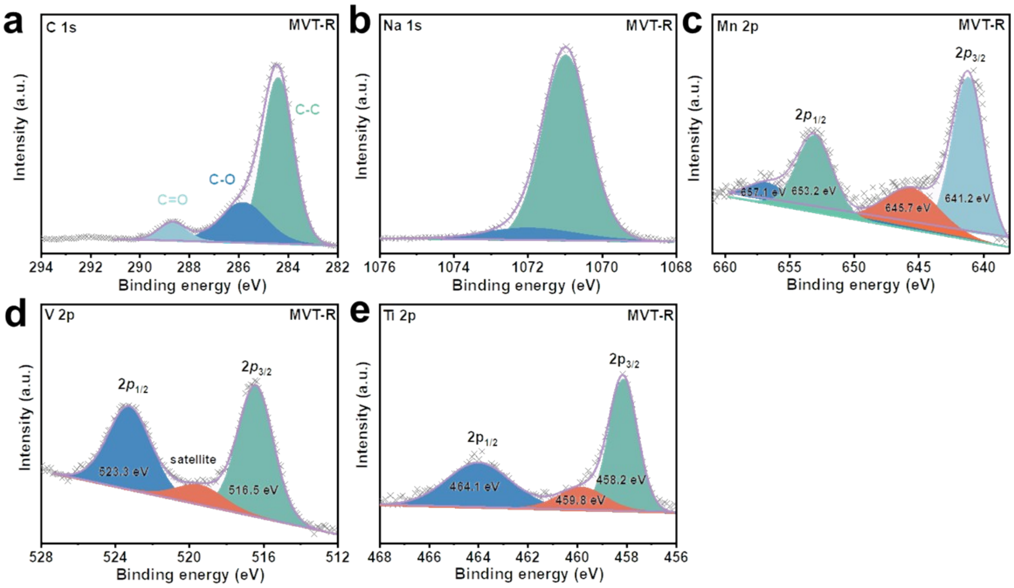

Figure S4 Fitted XPS spectra of (a) C 1s, (b) Na 1s, (c) Mn 2p, (d) V 2p and (f)Ti 2p for MVT cathode.

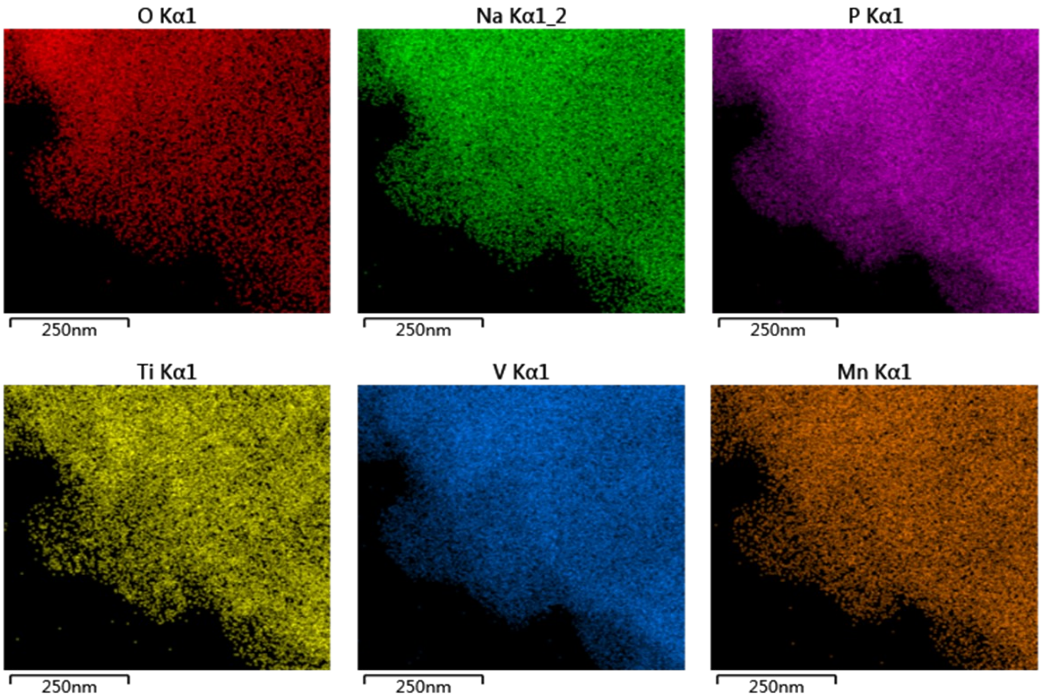

Figure S5 The elemental mappings of O, Na, P, Ti, V and Mn for MVT cathode.

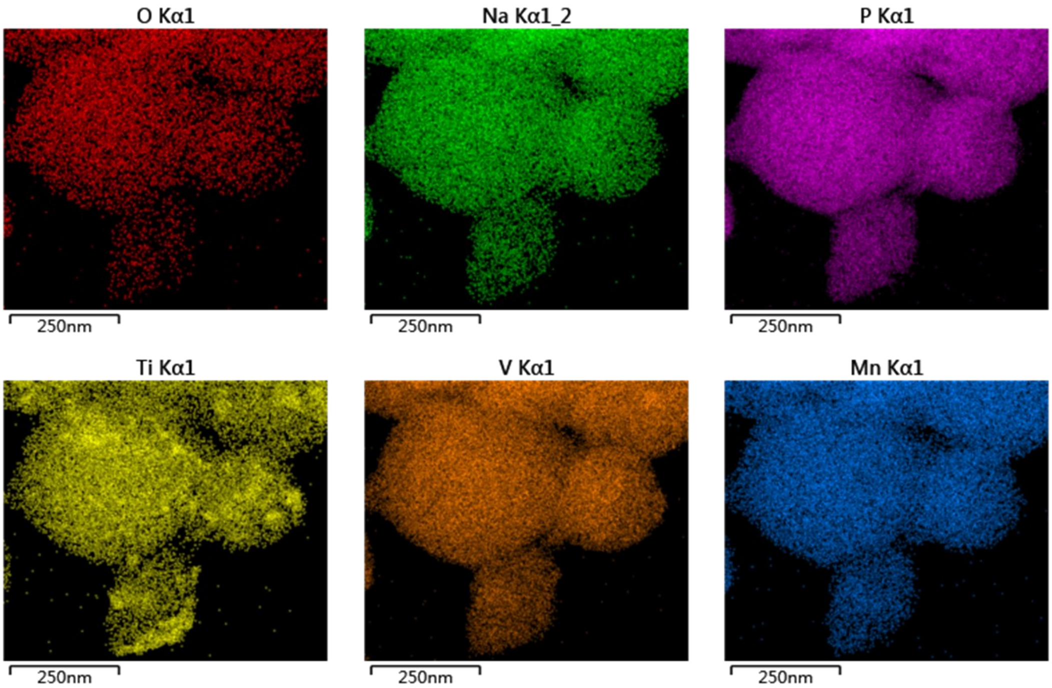

Figure S6 The elemental mappings of O, Na, P, Ti, V and Mn for MVT-R cathode.

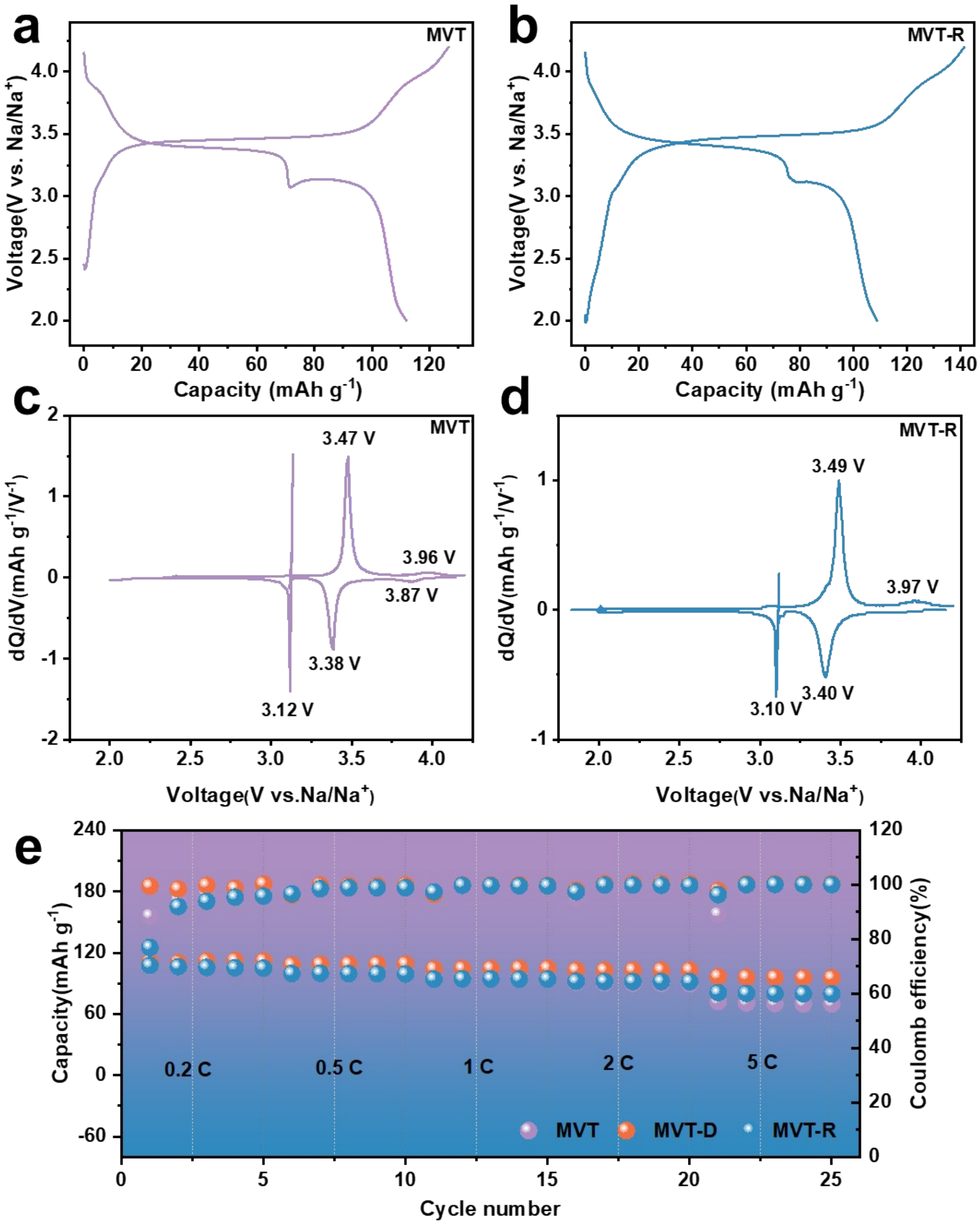

Figure S7 Electrochemical properties at low temperature of 0 °C. The charge/discharge profiles and dQ/dV curves of the initial cycle for (a, c) MVT, and (b, d) MVT-R cathodes. (e) Rate capabilities of MVT, MVT-D and MVT-R cathodes.

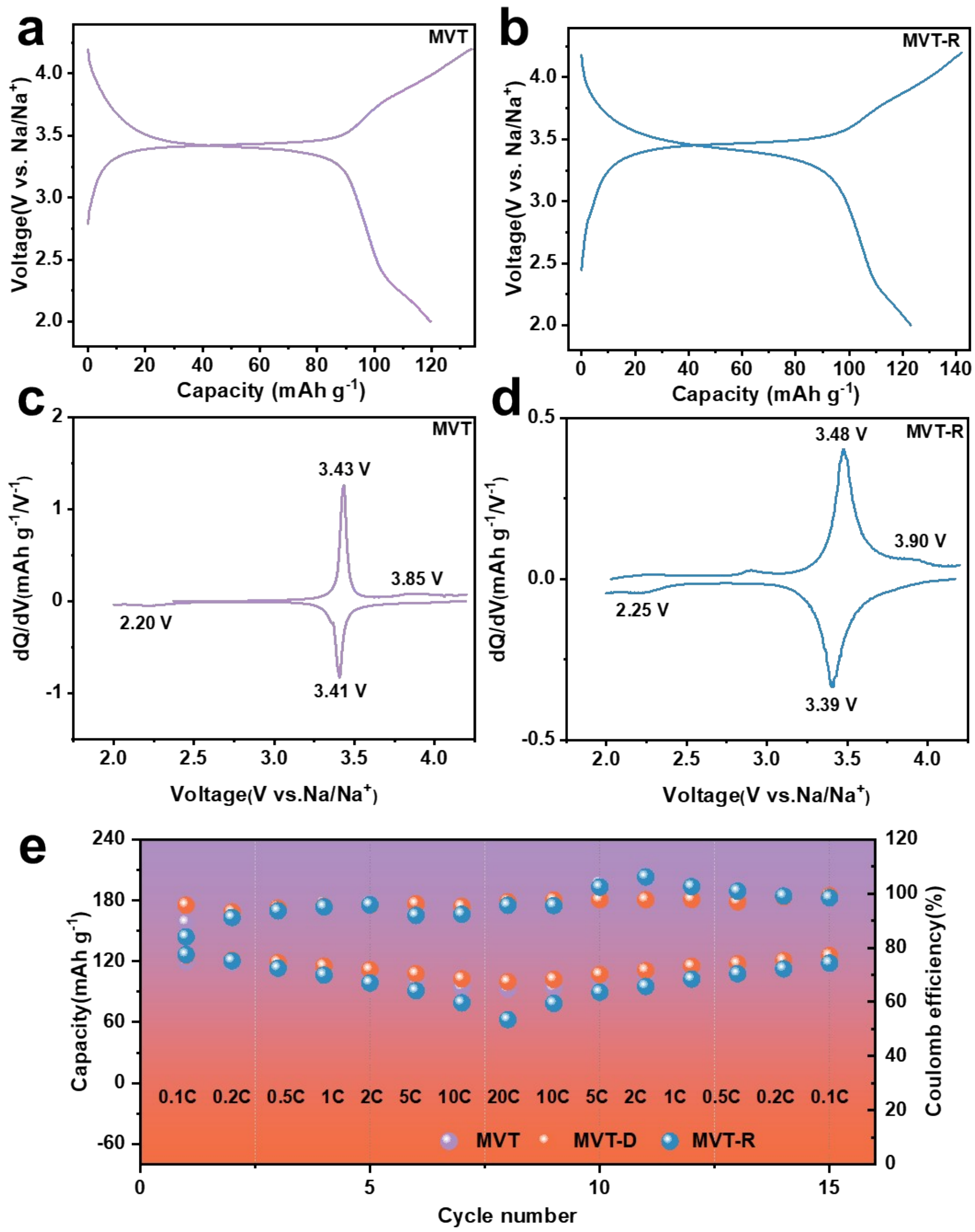

Figure S8 Electrochemical properties at high temperature of 55 °C. The charge/discharge profiles and dQ/dV curves of the initial cycle for (a, c) MVT, (b, d) MVT-R cathodes. (g) Rate capabilities of MVT, MVT-D and MVT-R cathodes. (h) Cycling performance of as-prepared samples at the current rate of 20 C.

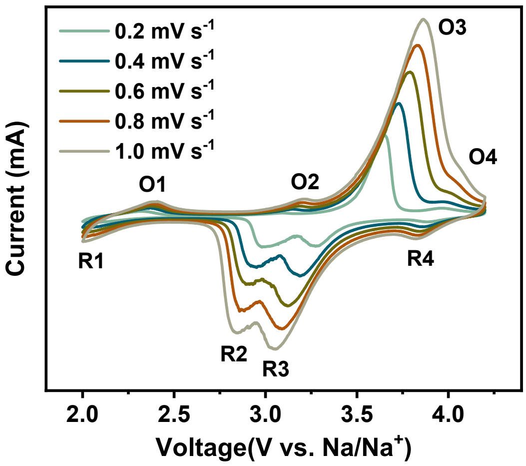

Figure S9 The cyclic voltammetry curves at varied scanning rates of 0.2, 0.4, 0.6, 0.8 and 1.0 mV s^{-1} for MVT-D cathode.

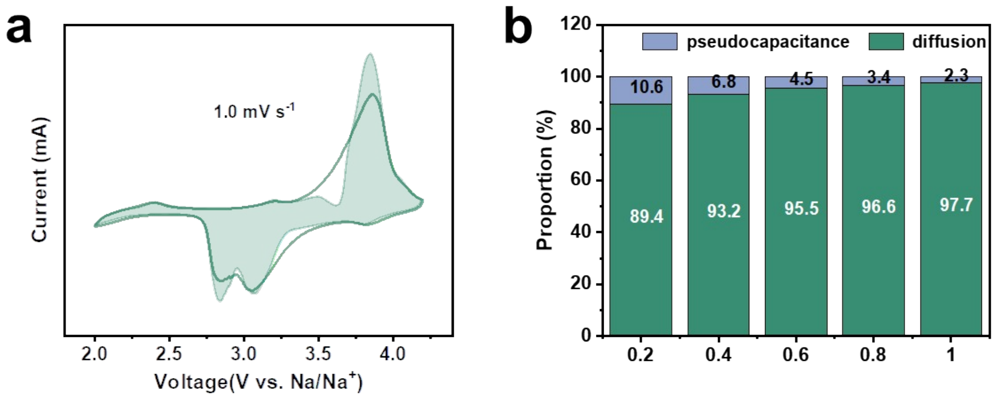

Figure S10 (a) The fitted curves of pseudocapacitance contribution for MVT-D cathode at the scanning rate at 1.0 mV s^{-1} and (b) the specific contribution values at varied scanning rates.

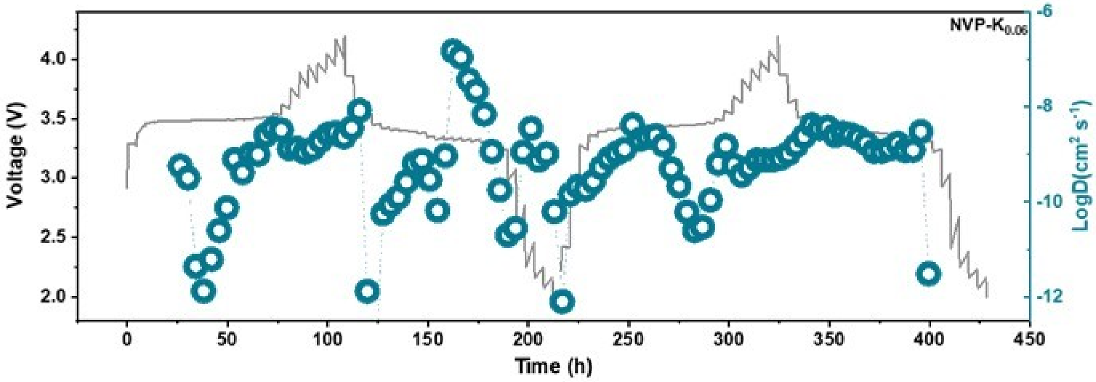

Figure S11 The GITT curves for MVT-D cathode for the initial two cycles

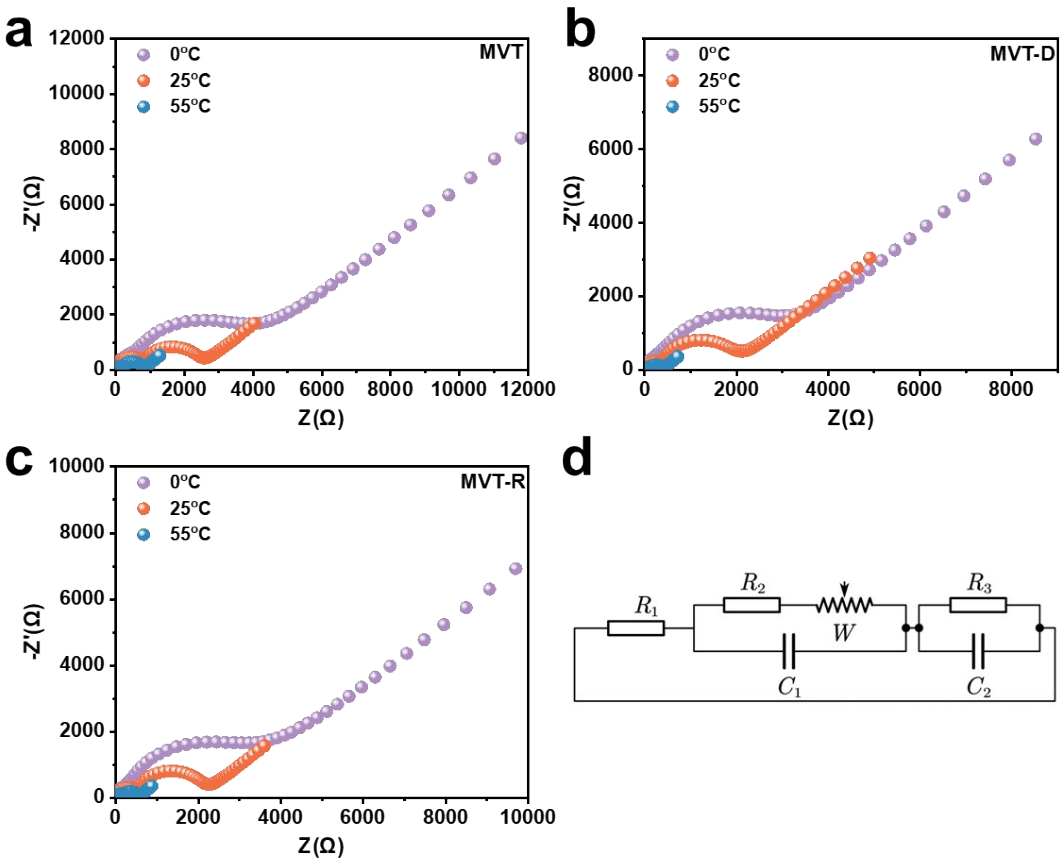

Figure S12 The fitted EIS plots of (a) MVT, (b) MVT-D and (c) MVT-R under different working temperatures at open circuit voltage. (d) The corresponding equivalent circuit for the EIS fitting.

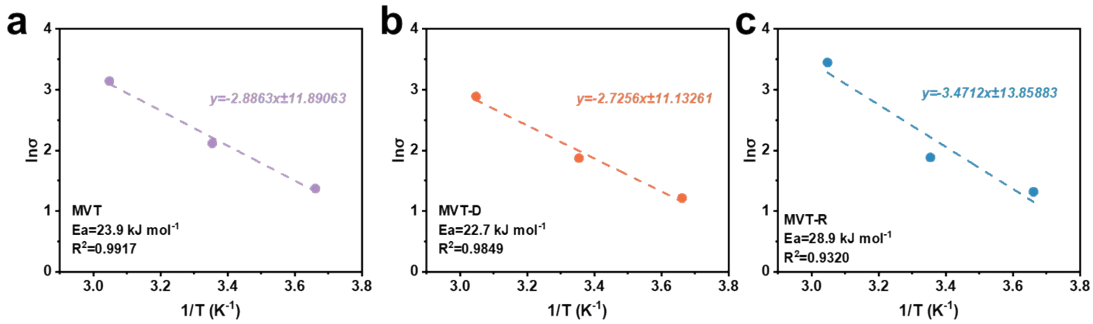

Figure S13 Arrhenius conductivity plots of (a) MVT, (b) MVT-D and (c) MVT-R cathodes.

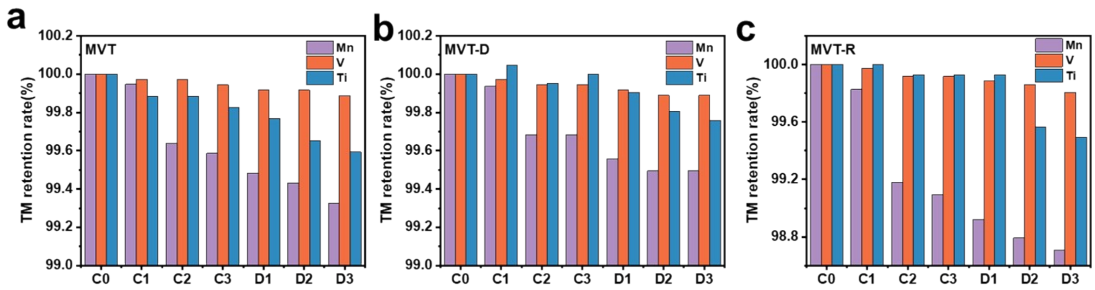

Figure S14 The transition metal retention rate of (a) MVT, (b) MVT-D and (c) MVT-R electrodes at varied charge-discharge states. Here, the mass values of active materials are almost the same at the beginning of these tests.

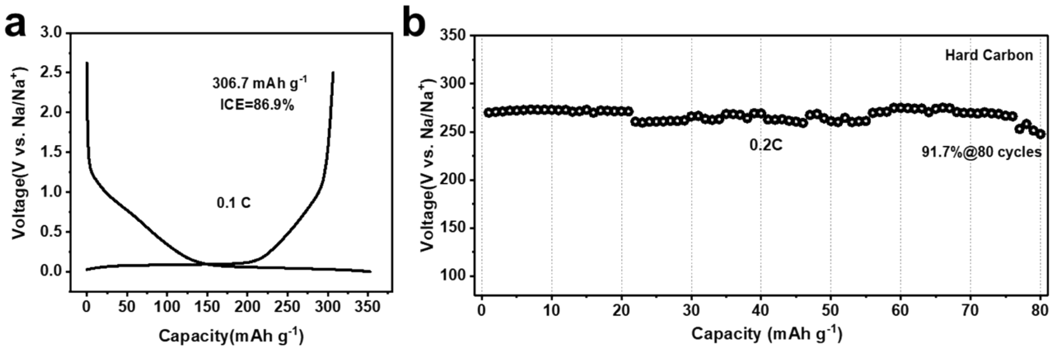

Figure S15 (a) The charge-discharge curves of commercial hard carbon anode at 0.1 C and (b) the corresponding cycling stability at 0.2 C.

Table S1 Crystallographic and Rietveld refinement parameters of as-synthesized samples derived from the GSAS software.

Spl.	**MVT**	**MVT-D**	**MVT-R**
Space group	$R\bar{3}c(167)$	$R\bar{3}c(167)$	$R\bar{3}c(167)$
Cell parameters	a=8.8762Å b=8.8762Å c=21.7265Å α=β=90° γ=120 ° V=1482.39Å^3	a=8.8622Å b=8.8622Å c=21.7179Å α=β=90° γ=120 ° V=1477.12Å^3	a=8.8891Å b=8.8891Å c=21.7315Å α=β=90° γ=120 ° V=1487.04Å^3
Reliability factors	R_{wp}=8.35% R_p=6.21% X^2=1.956	R_{wp}=7.59% R_p=6.14% X^2=1.995	R_{wp}=9.63% R_p=6.54% X^2=2.156

Table S2 Atomic coordinates, cation and anion occupancies of as-synthesized MVT cathode.

Element type	**Fractional coordinates**			**Site**	**Occu.**	**Uiso**
	x	**y**	**z**			
Na1	0.3333	0.6667	0.1667	6b	0.808(1)	0.0692(1)
Na2	0.6667	0.9735(6)	0.0833	18e	0.723(6)	0.0334(2)
O1	0.1432(1)	0.4929(9)	0.0778(7)	36f	0.996(1)	0.0035(8)
O2	0.5409(1)	0.8477(6)	-0.0258(1)	36f	0.998(1)	0.0371(1)
P1	-0.0423(6)	0.3333	0.0833	18e	0.993(7)	0.0273(6)
V1	0.3333	0.6667	0.0190	12c	0.5	0.0162(1)
Mn1	0.3333	0.6667	0.0190	12c	0.25	0.0136(9)
Ti1	0.3333	0.6667	0.0190	12c	0.25	0.0101(5)

Table S3 Atomic coordinates, cation and anion occupancies of as-synthesized MVT-D cathode.

Element type	**Fractional coordinates**			**Site**	**Occu.**	**Uiso**
	x	**y**	**z**			
Na1	0.3333	0.6667	0.1667	6b	0.801(3)	0.0884(6)
Na2	0.6667	0.9737(5)	0.0833	18e	0.718(1)	0.0442(2)
O1	0.1425(6)	0.4917(4)	0.0781(6)	36f	0.998(2)	0.0034(6)
O2	0.5378(1)	0.8435(2)	-0.0266(2)	36f	0.994(7)	0.0028(5)
P1	-0.0419(2)	0.3333	0.0833	18e	0.998(9)	0.0226(7)
V1	0.3333	0.6667	0.0190	12c	0.5	0.0014(5)
Mn1	0.3333	0.6667	0.0190	12c	0.2	0.0182(7)
Ti1	0.3333	0.6667	0.0190	12c	0.3	0.0115(6)

Table S4 Atomic coordinates, cation and anion occupancies of as-synthesized MVT-R cathode.

Element type	Fractional coordinates			Site	Occu.	Uiso
	x	y	z			
Na1	0.3333	0.6667	0.1667	6b	0.807(4)	0.0162(1)
Na2	0.6667	0.9732(8)	0.0833	18e	0.732(5)	0.0089(3)
O1	0.1417(7)	0.4916(6)	0.0778(6)	36f	0.999(1)	0.0132(5)
O2	0.5453(1)	0.8515(4)	-0.0262(0)	36f	0.993(9)	0.0056(4)
P1	-0.0431(0)	0.3333	0.0833	18e	0.994(1)	0.0123(6)
V1	0.3333	0.6667	0.0190	12c	0.5	0.0025(1)
Mn1	0.3333	0.6667	0.0190	12c	0.3	0.0120(1)
Ti1	0.3333	0.6667	0.0190	12c	0.2	0.0025(3)

Table S5 The ICP-MS results of the as-synthesized samples.

Samples	Na	Mn	V	Ti	P
MVT	2.982	0.521	0.978	0.481	3
MVT-D	2.813	0.413	0.991	0.601	3
MVT-R	3.232	0.596	1.023	0.412	3

Table S6 Multi-point BET results of the as-synthesized samples.

Samples	BET Surface Area (m^2/g)	Adsorption average pore diameter (nm)	Desorption average pore diameter (nm)
MVT	7.936	12.345	10.179
MVT-D	8.245	18.464	15.424
MVT-R	11.568	9.772	7.995

Table S7 The comparison of electrochemical performance for typical Mn-based cathodes for NIBs between the state-of-the-art literature and this work.

Cathode Materials	Rate Capabilities	Cycling Performance
$Na_{0.67}[Li_{0.21}Mn_{0.59}Ti_{0.2}]$[1]	1.5-4.5V 231 mAh g^{-1}@0.2 C/2.6V 195 mAh g^{-1}@0.5 C 170 mAh g^{-1}@1 C 147 mAh g^{-1}@2 C 120 mAh g^{-1}@5 C 2-4.5 V 121 mAh g^{-1}@0.2 C	1.5-4.5V 2 C, 100 cycles, 60.3% 2-4.5 V 2 C, 100 cycles, 67.4% 1C=100 mA g^{-1} 600.6 Wh kg^{-1}/0.2C
Tunnel typed-$Na_{0.44}Mn_{0.95}Mg_{0.05}O_2$[2]	2.0–3.8 V 105 mAh g^{-1} @0.2 C/3.0 V 99 mAh g^{-1} @0.5C 95 mAh g^{-1}@1 C 91 mAh g^{-1}@2 C 82 mAh g^{-1}@5 C 113 mAh g^{-1}@10 C 64 mAh g^{-1}@20 C 55 mAh g^{-1}@30 C	2 C, 800 cycles, 67% 1C=100 mA g^{-1} 315 Wh kg^{-1}/0.2C
P2-$Na_{7/9}Li_{1/9}Ni_{2/9}Mn_{5/9}Ti_{1/9}O_2$[3]	2.0–4.3 V 140 mAh g^{-1} @0.1 C /3.5 V 135 mAh g^{-1} @ 0.5C 132 mAh g^{-1} @1C 129 mAh g^{-1}@ 2C 122 mAh g^{-1}@ 5 C 115 mAh g^{-1}@10 C	1 C, 200 cycles, 90.2% 1C=100 mA g^{-1} 490 Wh kg^{-1}/0.1C

O3-$Na_{0.93}Li_{0.12}Ni_{0.25}Fe_{0.15}Mn_{0.48}O_2$[4]	2.0–4.2 V 130.1 mAh g^{-1}@ 20 mA g^{-1} /3.0V 92 mAh g^{-1}@ 2000 mA g^{-1}	16C, 200 cycles, 82.8% 390.3 Wh kg^{-1}/20 mA g^{-1}
O3-$NaNi_{0.5}Mn_{0.5}O_2$@P2-$Na_{2/3}MnO_2$[5]	2.0–4.0 V 141.4 mA h g^{-1} @ 0.1 C/3.0V	1C,150 cycles, 85.3% 5 C, 400 cycles,72% 424.2 Wh kg^{-1}/0.1C
$NaMn_3O_5$[6]	1.5–4.7 V 219 mAh g^{-1}@0.1 C/2.75V 210 mAh g^{-1}@0.2 C 197 mAh g^{-1}@0.5 C 183mAh g^{-1}@1 C 165 mAh g^{-1}@2 C 115 mAh g^{-1}@5C	0.1C, 20cycles, 70% (1 C = 200 mA g^{-1}) 602 Wh kg^{-1}/0.1C
P_2-type $Na_{0.6}Li_{0.2}Fe_{0.2}Mn_{0.6}O_2$[7]	2.0–4.4 V 167mAh g^{-1}@1/15 C/2.75V 161 mAh g^{-1}@0.1 C 145 mAh g^{-1}@0.2 C 135 mAh g^{-1}@0.4C 121 mAh g^{-1}@1 C 95 mAh g^{-1}@ 2C	1/15 C, 100 cycles, 78% 1C, 250 cycles, 70% (1 C = 250 mA g^{-1})
$Na_{0.66}Ni_{0.13}Mn_{0.54}Co_{0.13}O_2$[8] **(Ti-MNC)**	2.0–4.7 V 133.2 mAh g^{-1}@1 C/3.6 V 121 mAh g^{-1}@2 C 110 mAh g^{-1}@3 C 96 mAh g^{-1}@4 C 85 mAh g^{-1}@5 C 54 mAh g^{-1}@8C	1C, 100cycles,77.9 % (1 C = 200 mA g^{-1}) 456.4 Wh kg^{-1}/1C

	49 mAh g^{-1}@10 C	
P_2-type $Na_{0.58}Ni_{0.33}Mn_{0.67}O_{1.95}$[9]	2.6-4.5 V 61.3 mAh g^{-1}@1C/3.2V 3.8-4.5 V 18 mAh g^{-1}@1 C/3.95V 2.6-3.8 V 62 mAh g^{-1}@1 C/ 3.4 V 57 mAh g^{-1}@2 C 55 mAh g^{-1}@3 C 52 mAh g^{-1}@5 C	2.6-4.5 V 1C, 100 cycles, 16.7 % 3.8-4.5 V 1C, 100 cycles, 24 % 2.6-3.8 V 1C, 500 cycles, 94.5 % (1 C = 0.1 A g^{-1}) 2C, 500 cycles, 79.2 % 5C, 1000 cycles, 70.5 %
$Na_yFe_{0.4}Mn_{0.6}[Fe(CN)_6]$[10]	2.5–4.2 V 119 mAh g^{-1}@0.2 C/3.19 V 107 mAh g^{-1}@1 C 101 mAh g^{-1}@2 C 95 mAh g^{-1}@5 C 91 mAh g^{-1}@10 C 86 mAh g^{-1}@20 C 86 mAh g^{-1}@30 C	1 C, 100 cycles, 65% (1 C = 170 mA g^{-1}) 380 Wh kg^{-1}/0.2C
$Na_{1.38}Ni_{0.07}Mn_{0.93}[Fe(CN)_6]_{0.82}$[11] HCS-PBMN	2.5–4.2 V 123 mAh g^{-1}@0.5 C/3.31 V 109 mAh g^{-1}@1 C 100 mAh g^{-1}@2 C 89 mAh g^{-1}@ 6 C 76 mAh g^{-1}@ 8 C 61 mAh g^{-1}@ 16C 53 mAh g^{-1}@ 32 C	0.5 C, 600 cycles, 82.3% (1 C = 100 mA g^{-1}) 408 Wh kg^{-1}/0.5C
$Na_{1.6}Mn_{0.75}(Mn)_{0.25}[Fe(CN)_6]\cdot 1.97H_2O$[12]	2.5–4.2 V 137 mAh g^{-1}@0.25 C/3.2 V	5 C, 2700 cycles, 72.3% (1 C = 100 mA g^{-1})

		438 Wh kg^{-1}/0.25C
$Na_{1.6}Mn[Fe(CN)_6]_{0.9}$ PBM@NVOPF[13]	2.0–4.0 V 112.9 mAh g^{-1}@0.1 C/2.75V 104.6 mAh g^{-1}@0.5 C 101.7 mAh g^{-1}@1 C, 20 °C 109.5 mAh g^{-1}@1 C, 55 °C 98.9 mAh g^{-1}@2 C 95.4 mAh g^{-1}@5C 91.4 mAh g^{-1}@10C	1 C, 20 °C, 500 cycles, 84.3% 1 C, 55 °C, 200 cycles, 78.8% (1 C = 100 mA g^{-1})
$Na_{3.12}Mn_{2.44}(P_2O_7)_2$/C[14]	1.5–4.5 V 114 mAh g^{-1}@0.1 C/3.3V 104 mAh g^{-1}@0.2 C 98 mAh g^{-1}@0.5 C 92 mAh g^{-1}@1 C 82 mAh g^{-1}@2 C 68 mAh g^{-1}@5C 52 mAh g^{-1}@10 C	5 C, 500 cycles, 75% 376 Wh kg^{-1} / 0.1 C. (1 C = 120 mAh g^{-1}).
$Na_4Mn_2Co(PO_4)_2P_2O_7$/C -CNTs[15]	1.7–4.6 V 96.1 mAh g^{-1}@0.1 C/3.85 V 92.9 mAh g^{-1} @0.2C 83.6mAh g^{-1}@0.5C 74.4 mAh g^{-1}@1 C 61 mAh g^{-1}@2 C 49.1mAh g^{-1}@5 C 41 mAh g^{-1}@10 C	1 C, 150 cycles, 76.4%
$Na_4MnV(PO_4)_3$/C@Al($PO_3)_3$[16]	2.5–3.8 V 102 mAh g^{-1}@0.2 C/3.36V 97mAh g^{-1}@0.5 C	2.5–3.8V (3.52/3.253) 5 C, 3000 cycles, 88.5%

	94mAh g^{-1}@1 C 91 mAh g^{-1}@2 C 90 mAh g^{-1}@5 C 87mAh g^{-1}@10 C 83mAh g^{-1}@20 C 81mAh g^{-1}@30 C 75 mAh g^{-1}@40 C 61 mAh g^{-1}@50 C 2.5–4 V 111.6 mAh g^{-1}@0.2 C 50.8 mAh g^{-1} @10 C	10 C, 4000 cycles, 89.7% 2.5–4 V 5 C, 1000 cycles, 71.4%
$Na_{3.25}V_{1.75}Mn_{0.25}(PO_4)_3$/ C[17]	2.0–4.0 V 126 mAh g^{-1}@0.1 C /3.42V 119 mAh g^{-1}@0.2 C 113 bmAh g^{-1}@0.5 C 110 mAh g^{-1}@1 C 105 mAh g^{-1}@ 2 C 84 mAh g^{-1}@5 C	0.2 C, 40 cycles, 96% 1 C, 150 cycles, 89.3% (1 C = 100 mAh g^{-1}).
$Na_{4.5}Mn_{0.5}Fe_{0.5}Al(PO_4)_3$[18]	1.5–4.3 V 102 mAh g^{-1}@0.1 C/2.81V 88 mAh g^{-1}@0.2 C 73 mAh g^{-1}@0.5 C 60 mAh g^{-1}@1 C 40 mAh g^{-1}@2 C 35 mAh g^{-1}@5 C	0.2 C, 100 cycles, 60% (1 C = 117 mA g^{-1}) 287.7 Wh kg^{-1}/0.1 C
$Na_4Fe_{2.9}Mn_{0.1}Ti_{0.8}(PO_4)_2$ P_2O_7@C[19]	1.7–4.1 V 119.6 mAh g^{-1}@0.1 C/3.1 V 113.54 mAh g^{-1}@0.2 C 106.45 mAh g^{-1}@0.5 C	1 C, 100 cycles, 97.4 % 10C, 3000 cycles, 84.8 % (1 C = 129 mA g^{-1}) 370 Wh kg^{-1}

	101.76 mAh g^{-1}@1 C 96.68 mAh g^{-1}@2 C 88.97 mAh g^{-1}@5 C 81.66 mAh g^{-1}@10 C 72.18 mAh g^{-1}@20 C 64.39 mAh g^{-1}@30 C	
$Na_{3.5}MnTi(PO_4)_3$@MXene-rGO[20]	1.5–4.2 V 189 mAh g^{-1}@0.5 C/ 2.75V 183 mAh g^{-1}@1 C 173 mAh g^{-1}@2 C 150 mAh g^{-1}@6 C 122 mAh g^{-1}@10 C 101 mAh g^{-1}@15 C 97 mAh g^{-1}@20 C	10C, 2500 cycles, 75% 20C, 5000cycles, 82% (1 C = 0.1 A g^{-1}) 519.75 Wh kg^{-1}
Na_2MnPO_4F/Ti_3C_2-CQDs[21]	1.5–4.1 V 66 mAh g^{-1}@0.1 C/ 2.5 V 54 mAh g^{-1}@0.2 C 45 mAh g^{-1}@0.5 C 35 mAh g^{-1}@1 C 25 mAh g^{-1}@2 C 12 mAh g^{-1}@5 C	0.1 C, 100cycles, 90 % (1 C = 100 mA g^{-1}) 165 Wh kg^{-1}
$Na_3MnZr(PO_4)_3$[22]	2.5–4.25 V 107 mAh g^{-1}@0.1 C/ 3.53 V 100 mAh g^{-1}@0.2 C 89 mAh g^{-1}@0.5 C 81vmAh g^{-1}@1 C 74 mAh g^{-1}@2 C 59 mAh g^{-1}@5 C 52 mAh g^{-1}@10 C	0.5C, 500 cycles, 91% (1 C = 110 mA g^{-1}) 377 Wh kg^{-1}

$Na_4MnV(PO_4)_3$[23] **(NMVP)-D@cPANI**	2.5–3.8 V 102.5 mAh g^{-1}@0.2 C/3.4 V 98.5 mAh g^{-1}@0.5 C 96.1 mAh g^{-1}@1 C 93.7 mAh g^{-1}@2 C 90.5 mAh g^{-1}@5 C 85.8 mAh g^{-1}@10 C 77.8 mAh g^{-1}@20 C 73.8 mAh g^{-1}@30 C 69.1 mAh g^{-1}@40 C 61.68 mAh g^{-1}@50 C	0.2 C, 50 cycles, 94.5% (1 C = 110 mA g^{-1})
$Na_4MnV(PO_4)_3$[24]	2.5–3.8 V 104.5 mAh g^{-1}@0.2 C 103.5 mAh g^{-1}@0.5 C 102.1 mAh g^{-1}@1 C 101.3 mAh g^{-1}@2 C 100.0 mAh g^{-1}@5 C 98.5 mAh g^{-1}@10 C 96.2 mAh g^{-1}@20 C 94.4 mAh g^{-1}@30 C 91.0 mAh g^{-1}@50 C 85.6 mAh g^{-1}@75 C 82.4 mAh g^{-1}@100 C	5 C, 1000 cycles, 94.4% (1 C = 110 mA g^{-1})
$Na_4VMn_{0.5}Fe_{0.5}(PO_4)_3$[25]	2.0–4.0 V 122.6 mAh g^{-1}@0.5 C 118.5 mAh g^{-1}@1 C 113.9 mAh g^{-1}@3 C 109.3 mAh g^{-1}@5 C 107.6 mAh g^{-1}@10 C 100.6 mAh g^{-1}@20 C	2.0–3.8 V 20 C, 3000 cycles, 94% (1 C = 110 mA g^{-1})

$Na_4V_{0.8}Al_{0.2}Mn(PO_4)_3$[26]	2.5–3.8 V 92.9 mAh g^{-1}@0.2 C 90.8 mAh g^{-1}@0.5 C 87.8 mAh g^{-1}@1 C 87.7 mAh g^{-1}@2 C 87.7 mAh g^{-1}@5 C 84.7 mAh g^{-1}@10C 83.6 mAh g^{-1}@20 C 83.5 mAh g^{-1}@30 C 83.4 mAh g^{-1}@40 C	5 C, 1000 cycles, 92% (1 C = 110 mA g^{-1})
This work **$Na_{2.8}Mn_{0.4}V_{1.0}Ti_{0.6}(PO_4)_3$**	**2-4.2V** **126.2mAh/g / 3.41V**	**20C, 3000 cycles, 88.1%** **430 Wh kg^{-1}/0.1C**

Table S8 The comparison of electrochemical performance under wide-temperature conditions for NASICON-type cathodes between the state-of-the-art literature and this work.

Cathode Materials	Reversible Capacity	Working Temp.	Cycling Performance
$Na_3V_2(PO_4)_3$[27]	116 mAh g^{-1}	55 °C	/
	111 mAh g^{-1}	-20 °C	10 C, 75.8%, 500 cycles
$Na_4Fe_3(PO_4)_2P_2O_7$[28]	145.1 mAh g^{-1}	80 °C	3 A g^{-1} 65%,200 cycles
	130.3 mAh g^{-1}	-40 °C	80 mA g-1 92%,120 cycles
$Na_3V_{2-x-y}Cr_xMg_y(PO_4)_3$[29]	100 mAh g^{-1}	55 °C	100 mA g^{-1} 88%,100 cycles
	70 mAh g^{-1}	-10 °C	100 mA g^{-1} 88.7%,50 cycles
$Na_{3.5}Mn_{0.5}V_{1.5}(PO_4)_3$[30]	86.5 mAh g^{-1}	50 °C	/
	61.4 mAh g^{-1}	-20 °C	/
$Na_3V(PO_3)_3N$[31]	78 mAh g^{-1}	50 °C	1 C, 86.4%, 800 cycles
	59 mAh g^{-1}	-15 °C	1 C, 92.3%, 800 cycles
$Na_3V_2(PO_4)_2O_2F_{0.99}Cl_{0.01}$[32]	128 mAh g^{-1}	50 °C	0.5 C, 70%, 100 cycles
	88.9 mAh g^{-1}	-25 °C	0.5 C, 95.8%, 100 cycles
$Na_3V_{1.94}K_{0.06}(PO_4)_3$[33]	127.8 mAh g^{-1}	55 °C	20 C, 99.5%, 1500 cycles

	90.9 mAh g^{-1}	-30 ^{o}C	0.2 C, 96.9% 200 cycles
$Na_{2.8}Mn_{0.4}VTi_{0.6}(PO_4)_3$ This work	**128.1 mAh g^{-1}**	**55 ^{o}C**	**20 C, 80.2%, 1500 cycles**
	114.6 mAh g^{-1}	**0 ^{o}C**	**1 C, 93.5% 500 cycles**

Table S9 The valence information of Mn, V and Ti for MVT-D cathode analyzed by ex situ XPS spectra and ICP results. (Note that: The Mn2+ ions on the surface were easily oxidized during the XPS testing process, thus the combination of XPS and ICP results based on charge conservation and material conservation was used to confirm the accurate chemical valence for the as-prepared MVT-D cathode at varied states.)

Elements	**Mn**			**V**			**Ti**	
Valence	**Mn^{2+}**	**Mn^{3+}**	**Mn^{4+}**	**V^{3+}**	**V^{4+}**	**V^{5+}**	**Ti^{3+}**	**Ti^{4+}**
C0	100%	0	0	100%	0	0	0	100%
C1	65%	35%	0	47%	53%	0	0	100%
C2	0	100%	0	0	100%	0	0	100%
C3	0	100%	0	0	46%	54%	0	100%
D1	8%	92%	17.17	0	100%	0	0	100%
D2	67%	33%	17.15	59%	41%	0	0	100%
D3	100%	0	17.14	100%	0	0	21%	79%

According to these results, the chemical valences of Mn, V and Ti were 2, 3 and 4, respectively, for the pristine electrode, while they changed to 3, 4.54 and 3.79 after the charge-discharge process, which means the total number of the transferred electrons is: (3-2)*0.4+(4.54-3)*1+(4-3.79)*0.6=2.066. Based on the number of electrons transferred, the capacity contributions for Mn, V and Ti elements are 19.4%, 74.5% and 6.1%, respectively.

Table S10 The ICP-MS results of electrodes at varied charge-discharge states.

Samples	MVT			MVT-D			MVT-R		
Element	**Mn**	**V**	**Ti**	**Mn**	**V**	**Ti**	**Mn**	**V**	**Ti**
C0	19.32	35.67	17.21	15.81	36.12	20.61	23.19	36.05	13.82
C1	19.3	35.66	17.19	15.8	36.11	20.62	23.15	36.04	13.82
C2	19.21	35.66	17.19	15.76	36.1	20.60	23.00	36.02	13.81
C3	19.19	35.65	17.18	15.76	36.1	20.61	22.98	36.02	13.81
D1	19.18	35.64	17.17	15.74	36.09	20.59	22.94	36.01	13.81
D2	19.16	35.64	17.15	15.73	36.08	20.57	22.91	36.00	13.76
D3	19.14	35.63	17.14	15.73	36.08	20.56	22.89	35.98	13.75

Table S11 Comparison of the MVT-D-based full cell electrochemical performance with other related state-of-the-art configurations.

Cathode Materials	Anodes	Rate capabilities	Capacity retention
MNVP@C NWs[34]	HC	78.8 mAh g^{-1} @11 A g^{-1} (2.3−3.8 V)	85.7%@5 C 8000 cycles
NVP@C NPs[35]	HC	105 mAh g^{-1} @59 mA g^{-1} (2.0−4.0 V)	57%@0.5 C 100 cycles
NVP@C microspheres[36]	SnS	62 mAh g^{-1} @2 A g^{-1} (1.0−3.7 V)	74.6%@0.2 A g^{-1} 500 cycles
NVP@C[37]	Sn	80 mAh g^{-1} @10 A g^{-1} (1.9−4.0 V)	90%@10 A g^{-1} 5000 cycles
Fe-doped NVPF/NVP[38]	CuS	90 mAh g^{-1}@3C (0−4.25 V)	88%@10C 800 cycles
NFPP-E@C[39]	Fe_3O_4	227 mAh g^{-1}@100 mA g^{-1} (0.1−4.0 V)	76.9%@100 mA g^{-1} 500 cycles
NVP-NFPP@C@G[40]	HC	111.5 mAh g^{-1}@0.1C (2.0−4.3 V)	87.2%@2C 100 cycles
NVFP[41]	HC	102.5 mAh g^{-1}@0.1C (2.0−4.3 V)	92%@2C 500 cycles
Na-rich-NMTVP[42]	HC	137.3 mAh g^{-1}@100 mA g^{-1} (1.5−4.3 V)	86.4%@100 mA g^{-1} 96 cycles

Na-deficient NMVTP (This work)	**HC**	**122.2 mAh g^{-1}@0.1C (2.0−4.2 V)**	94.6%@2C 150 cycles

References

1. H. Xu, C. Cheng, S. Chu, X. Zhang, J. Wu, L. Zhang, S. Guo and H. Zhou, *Adv. Funct. Mater.*, 2020, **30**, 2005164.
2. X.-L. Li, J. Bao, Y.-F. Li, D. Chen, C. Ma, Q.-Q. Qiu, X.-Y. Yue, Q.-C. Wang and Y.-N. Zhou, *Adv. Sci.*, 2021, **8**, 2004448.
3. T. Zhang, H. Ji, X. Hou, W. Ji, H. Fang, Z. Huang, G. Chen, T. Yang, M. Chu, S. Xu, Z. Chen, C. Wang, W. Yang, J. Yang, X. Ma, K. Sun, D. Chen, M. Tao, Y. Yang, J. Zheng, F. Pan and Y. Xiao, *Nano Energy*, 2022, **100**, 107482.
4. X.-G. Yuan, Y.-J. Guo, L. Gan, X.-A. Yang, W.-H. He, X.-S. Zhang, Y.-X. Yin, S. Xin, H.-R. Yao, Z. Huang and Y.-G. Guo, *Adv. Funct. Mater.*, 2022, **32**, 2111466.
5. X. Liang, T.-Y. Yu, H.-H. Ryu and Y.-K. Sun, *Energy Storage Mater.*, 2022, **47**, 515-525.
6. S. Guo, H. Yu, Z. Jian, P. Liu, Y. Zhu, X. Guo, M. Chen, M. Ishida and H. Zhou, *ChemSusChem*, 2014, **7**, 2115-2119.
7. Z. Ding, Y. Liu, Q. Tang, Q. Jiang, J. Lu, Z. Xiao, P. Yao, M. Monasterio, J. Wu and X. Liu, *Electrochim. Acta*, 2018, **292**, 871-878.
8. Q. Zhao, F. K. Butt, Z. Guo, L. Wang, Y. Zhu, X. Xu, X. Ma and C. Cao, *Chem. Eng. J.*, 2021, **403**, 126308.
9. X. Cai, Y. Xu, L. Meng, X. Wei, F. Xiong, T. Xiong and Q. An, *J. Alloys Compd.*, 2020, **820**, 153093.
10. W. Gong, R. Zeng, S. Su, M. Wan, Z. Rao, L. Xue and W. Zhang, *J. Nanopart. Res.*, 2019, **21**, 274.
11. Y. Huang, M. Xie, Z. Wang, Y. Jiang, Y. Yao, S. Li, Z. Li, L. Li, F. Wu and R. Chen, *Small*, 2018, **14**, 1801246.
12. Y. Shang, X. Li, J. Song, S. Huang, Z. Yang, Z. J. Xu and H. Y. Yang, *Chem*, 2020, **6**, 1804-1818.
13. F. Peng, L. Yu, S. Yuan, X.-Z. Liao, J. Wen, G. Tan, F. Feng and Z.-F. Ma, *ACS Appl. Mater. Interf.*, 2019, **11**, 37685-37692.
14. H. Li, Z. Zhang, M. Xu, W. Bao, Y. Lai, K. Zhang and J. Li, *ACS Appl. Mater. Interf.*, 2018, **10**, 24564-24572.

15. L. Tang, X. Liu, Z. Li, X. Pu, J. Zhang, Q. Xu, H. Liu, Y.-G. Wang and Y. Xia, *ACS Appl. Mater. Interf.*, 2019, **11**, 27813-27822.
16. K. Wang, X. Huang, C. Luo, Y. Shen, H. Wang and T. Zhou, *J. Colloid Interface Sci.*, 2023, **642**, 705-713.
17. X. Lin, X. Ren, L. Cong, Y. Liu and X. Xiang, *ChemElectroChem*, 2022, **9**, e202200669.
18. X.-H. Liu, W.-H. Lai, J. Peng, Y. Gao, H. Zhang, Z. Yang, X.-X. He, Z. Hu, L. Li, Y. Qiao, M.-H. Wu and H.-K. Liu, *Carbon Neutralization*, 2022, **1**, 49-58.
19. Q. Tao, H. Ding, X. Tang, K. Zhang, J. Teng, H. Zhao and J. Li, *Energy Fuels*, 2023, **37**, 6230-6239.
20. H. Zhang, L. Shen, X. Geng, J. Zhang, Y. Jiang, H. Ma, Q. Liu, K. Yang, J. Ma and N. Zhu, *Chem. Eng. J.*, 2023, **466**, 143132.
21. D. Sun, R. Guo, Y. Lv, W. Li, M. Lu, Q. Wei, Z. Liu and G.-C. Han, *Diamond Relat. Mater.*, 2022, **128**, 109216.
22. H. Gao, I. D. Seymour, S. Xin, L. Xue, G. Henkelman and J. B. Goodenough, *J. Am. Chem. Soc.*, 2018, **140**, 18192-18199.
23. K. Wang, X. Huang, C. Luo, Z. Zhang, H. Wang and T. Zhou, *ACS Appl. Energy Mater.*, 2022, **5**, 15701-15709.
24. L. Zhu, M. Zhang, L. Yang, K. Zhou, Y. Wang, D. Sun, Y. Tang and H. Wang, *Nano Energy*, 2022, **99**, 107396.
25. C. Xu, J. Zhao, E. Wang, X. Liu, X. Shen, X. Rong, Q. Zheng, G. Ren, N. Zhang, X. Liu, X. Guo, C. Yang, H. Liu, B. Zhong and Y.-S. Hu, *Adv. Energy Mater.*, 2021, **11**, 2100729.
26. C. Xu, R. Xiao, J. Zhao, F. Ding, Y. Yang, X. Rong, X. Guo, C. Yang, H. Liu, B. Zhong and Y.-S. Hu, *ACS Energy Lett.*, 2022, **7**, 97-107.
27. T. Liu, B. Wang, X. Gu, L. Wang, M. Ling, G. Liu, D. Wang and S. Zhang, *Nano Energy*, 2016, **30**, 756-761.
28. Z. Li, Y. Zhang and Y. Wang, *SmartMat*, 2023, e1191, DOI:10.1002/smm2.1191.
29. P. B. Madambikkattil, S. V. Nair and D. Santhanagopalan, *ACS Appl. Energy Mater.*, 2022, **5**, 10473-10482.

30. X. Ma, X. Cao, Y. Zhou, S. Guo, X. Shi, G. Fang, A. Pan, B. Lu, J. Zhou and S. Liang, *Nano Res.*, 2020, **13**, 3330-3337.
31. M. Chen, W. Hua, J. Xiao, D. Cortie, X. Guo, E. Wang, Q. Gu, Z. Hu, S. Indris and X. L. Wang, *Angew. Chem. Int. Ed.*, 2020, **132**, 2470-2477.
32. Z.-Y. Gu, J.-Z. Guo, Z.-H. Sun, X.-X. Zhao, X.-T. Wang, H.-J. Liang, X.-L. Wu and Y. Liu, *Cell Reports Physical Science*, 2021, **2**, 100665.
33. X. Shen, M. Han, Y. Su, M. Wang and F. Wu, *Nano Energy*, 2023, **114**, 108640.
34. L. Liang, X. Li, F. Zhao, J. Zhang, Y. Liu, L. Hou and C. Yuan, *Adv. Energy Mater.*, 2021, **11**, 2100287.
35. W. Ren, X. Yao, C. Niu, Z. Zheng, K. Zhao, Q. An, Q. Wei, M. Yan, L. Zhang and L. Mai, *Nano Energy*, 2016, **28**, 216-223.
36. X. Cao, A. Pan, B. Yin, G. Fang, Y. Wang, X. Kong, T. Zhu, J. Zhou, G. Cao and S. Liang, *Nano Energy*, 2019, **60**, 312-323.
37. M. K. Sadan, H. Kim, C. Kim, S. H. Cha, K.-K. Cho, K.-W. Kim, J.-H. Ahn and H.-J. Ahn, *J. Mater. Chem. A*, 2020, **8**, 9843-9849.
38. J. Y. Park, Y. Shim, Y.-i. Kim, Y. Choi, H. J. Lee, J. Park, J. E. Wang, Y. Lee, J. H. Chang, K. Yim, C. W. Ahn, C.-W. Lee, D. K. Kim and J. M. Yuk, *J. Mater. Chem. A*, 2020, **8**, 20436-20445.
39. M. Chen, W. Hua, J. Xiao, D. Cortie, W. Chen, E. Wang, Z. Hu, Q. Gu, X. Wang, S. Indris, S.-L. Chou and S.-X. Dou, *Nat. Commun.*, 2019, **10**, 1480.
40. J.-Z. Guo, H.-X. Zhang, Z.-Y. Gu, M. Du, H.-Y. Lü, X.-X. Zhao, J.-L. Yang, W.-H. Li, S. Kang, W. Zou and X.-L. Wu, *Adv. Funct. Mater.*, 2022, **32**, 2209482.
41. X.-X. Zhao, W. Fu, H.-X. Zhang, J.-Z. Guo, Z.-Y. Gu, X.-T. Wang, J.-L. Yang, H.-Y. Lü, X.-L. Wu and E. H. Ang, *Adv. Sci.*, 2023, **10**, 2301308.
42. P. Hu, T. Zhu, C. Cai, X. Wang, L. Zhang, L. Mai and L. Zhou, *Angew. Chem. Int. Ed.*, 2023, **62**, e202219304.